

## Electronic Supplementary Information (ESI)

### Achiral Isomers controlled Circularly Polarized Luminescence in Supramolecular Hydrogels

Li Yang,<sup>a</sup> Fang Wang,<sup>a</sup> Dang-i Y. Auphedeous,<sup>a</sup> Chuan-Liang Feng\*<sup>ab</sup>

<sup>a</sup> State key Lab of Metal Matrix Composites, School of Materials Science and Engineering, Shanghai Jiao Tong University, Dongchuan Road 800, 200240, Shanghai, China.

<sup>b</sup> Collaborative Innovation Center of Nano Function Materials & Application, Key Lab For Special Functional Materials, Ministry of Education, Henan University, 475004, Kaifeng, China.

E-mail: clfeng@sjtu.edu.cn

#### 1. Supplementary Figures

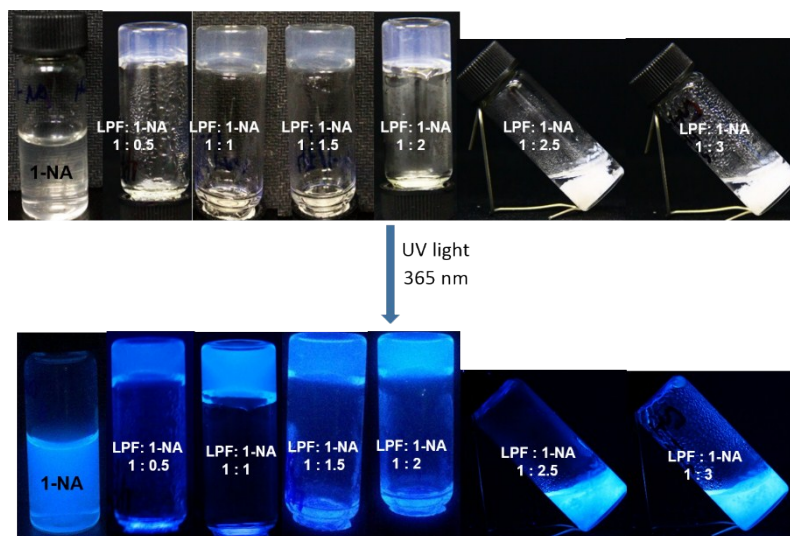


**Figure S1.** Photo images of co-assemblies of LPF with 1NA with different molar ratio before and after UV irradiation (365 nm) with the total gelators concentration of 0.2 wt%. 1NA could not form hydrogels in H<sub>2</sub>O.

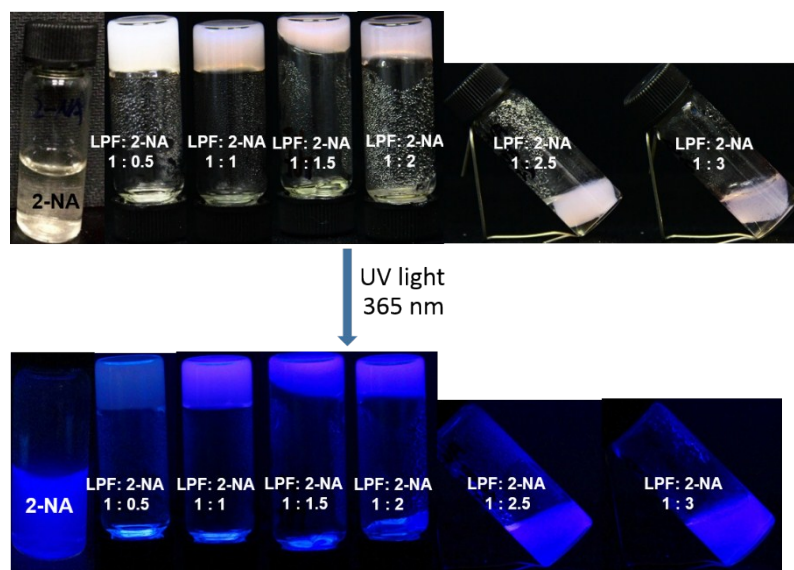


**Figure S2.** Photo images of co-assemblies of LPF with 2NA with different molar ratio before and after UV irradiation (365 nm) with the total gelators concentration of 0.2 wt%. 2NA could not form hydrogels in H<sub>2</sub>O.

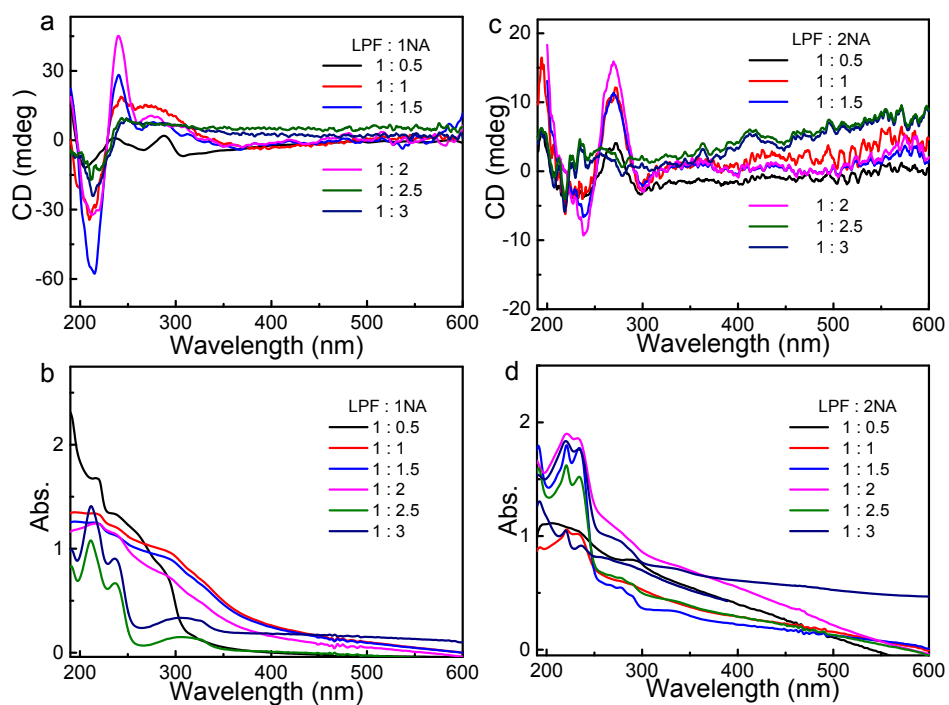


**Figure S3.** CD and UV/Vis spectra of (a)(b) LPF-1NA and (c)(d) LPF-2NA at different molar ratios with the total gelators concentration of 0.2 wt%.

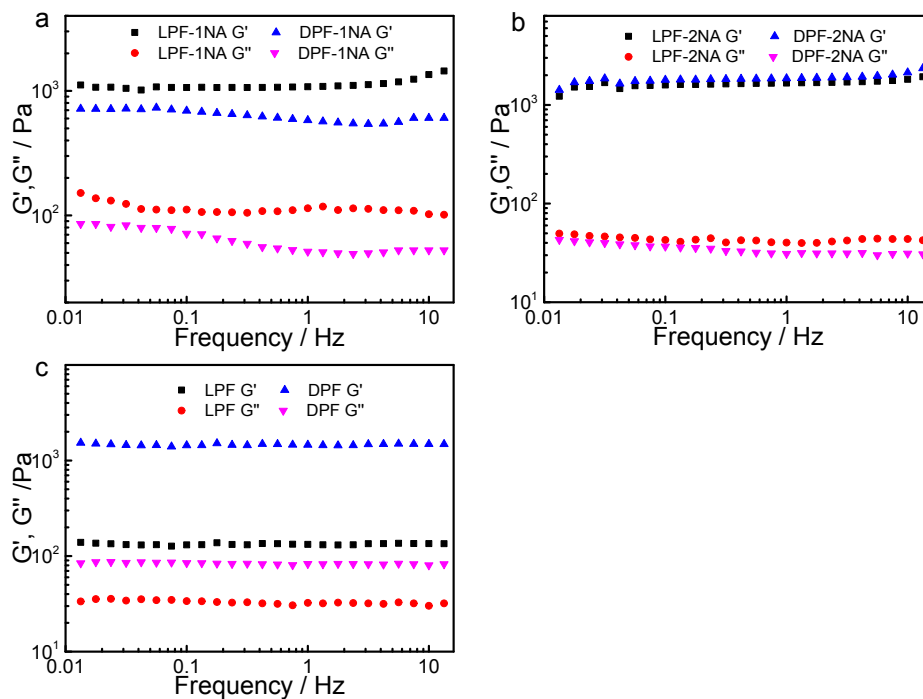


**Figure S4.** Rheological measurement of the frequency sweep at a strain of 1% of PF-1NA, PF-2NA and PF hydrogels with the total gelators concentration of 0.2 wt%.

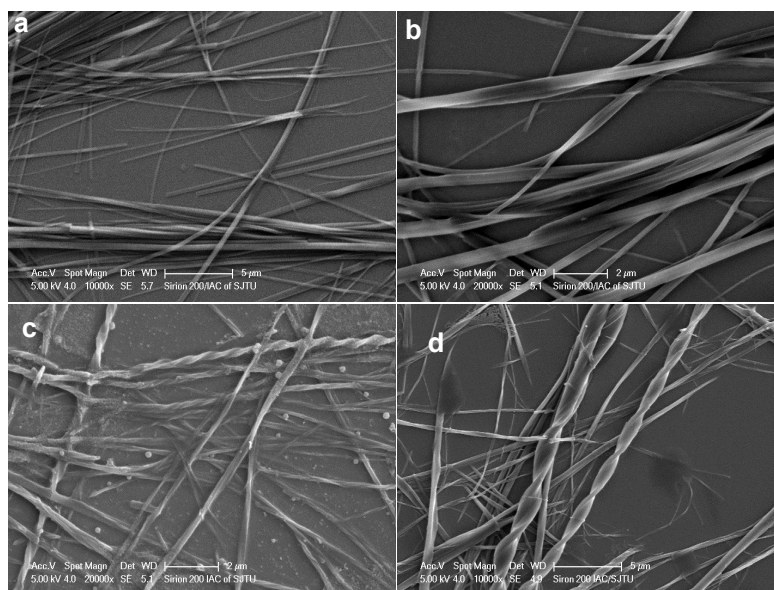


**Figure S5.** SEM images of coassemblies of (a) LPF:1NA = 1 : 1, (b) DPF:1NA = 1 : 1, (c) LPF:2NA = 1 : 1 and (d) DPF:2NA = 1 : 1.

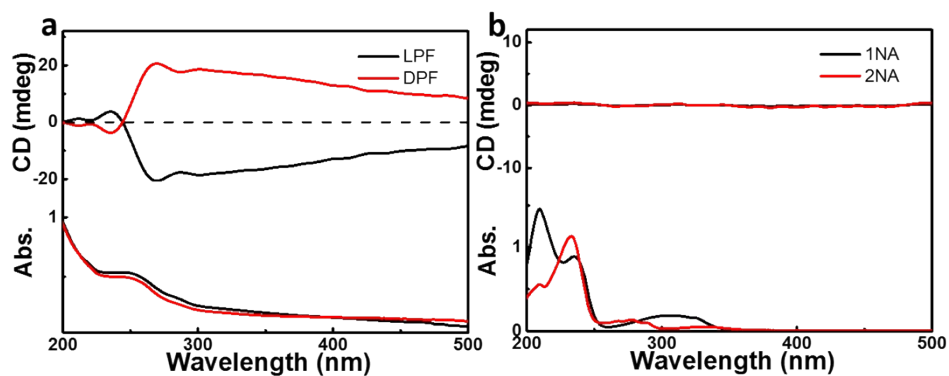


**Figure S6.** CD and UV/Vis spectra of (a) LPF and DPF hydrogels (with the concentration of LPF/DPF at  $2.0 \text{ mg mL}^{-1}$ ), (b) 1NA, 2NA in aqueous solution (with the concentration of  $0.54 \text{ mg mL}^{-1}$ ). Although obvious UV absorption of 1NA and 2NA were observed at 210nm and 220 nm respectively, their CD curves display chirality silence, indicating the non-chirality of 1NA and 2NA.

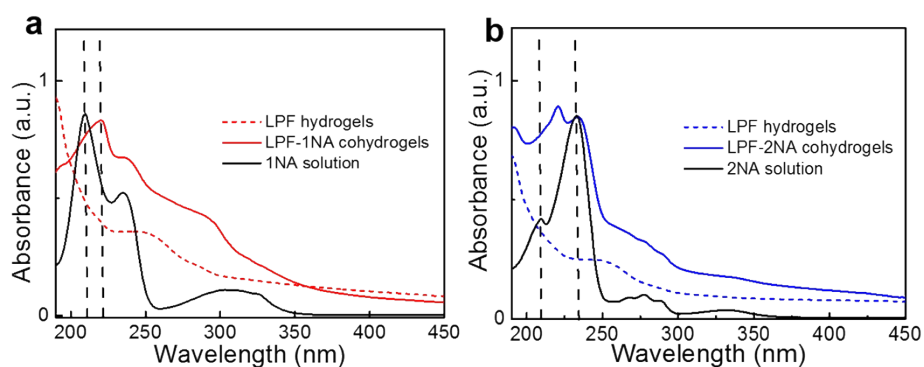


**Figure S7.** UV/Vis spectra of (a) LPF hydrogels, LPF-1NA cohydrogels, 1NA in aqueous solution (with the concentration of  $0.54 \text{ mg mL}^{-1}$ ) (b) LPF hydrogels, LPF-2NA cohydrogels, 2NA in aqueous solution (with the concentration of  $0.54 \text{ mg mL}^{-1}$ ), hydrogels with the total gelators concentration of 0.2 wt%.

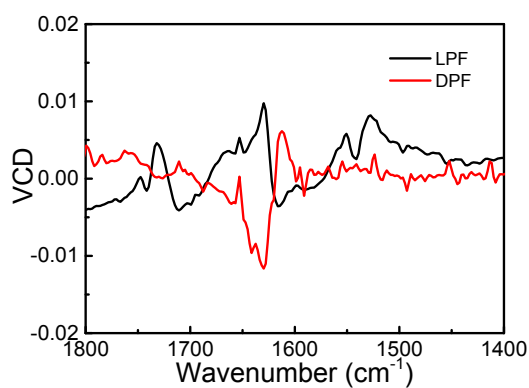


**Figure S8.** VCD spectra of LPF and DPF hydrogels.

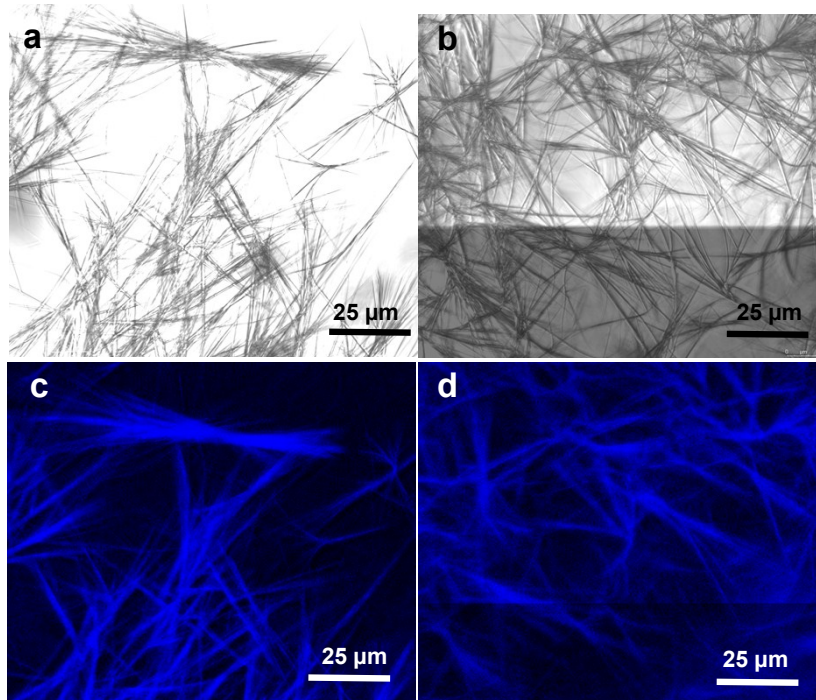


**Figure S9.** Optical microscopy and laser scanning confocal microscopy images of (a)(c) DPF-1NA and (b)(d) DPF-2NA.

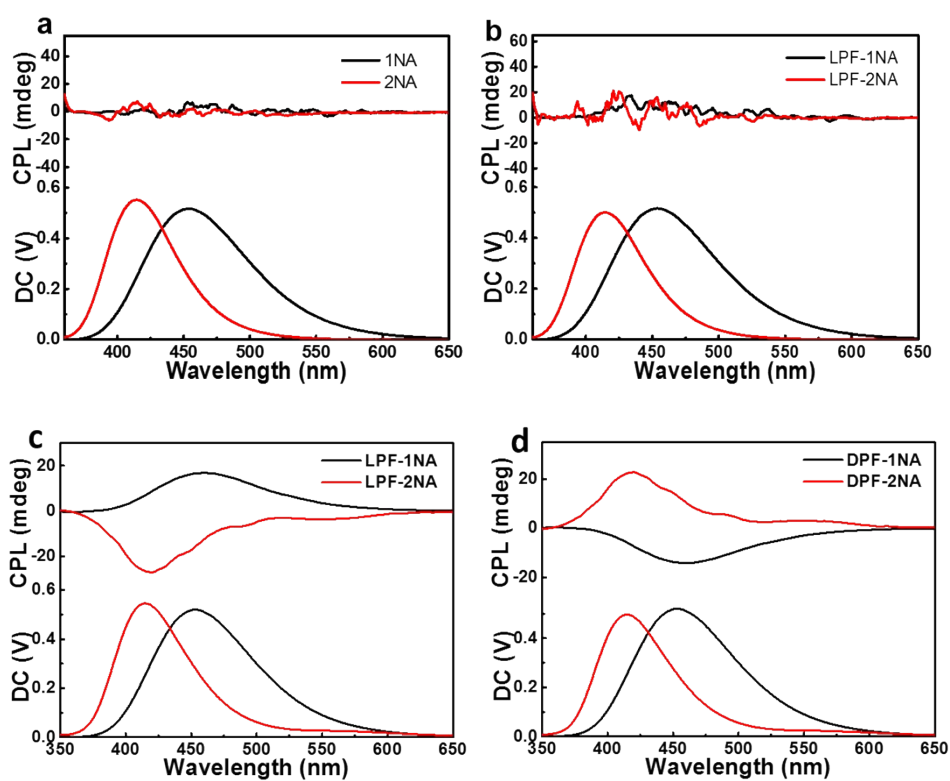


**Figure S10.** CPL spectra excited at 325 nm of (a) 1NA, 2NA in aqueous solution, (b) LPF-1NA and LPF-2NA in aqueous solution, coassemblies at molar ratio of 1:1 (c) LPF-1NA/2NA and (d) DPF-1NA/2NA.

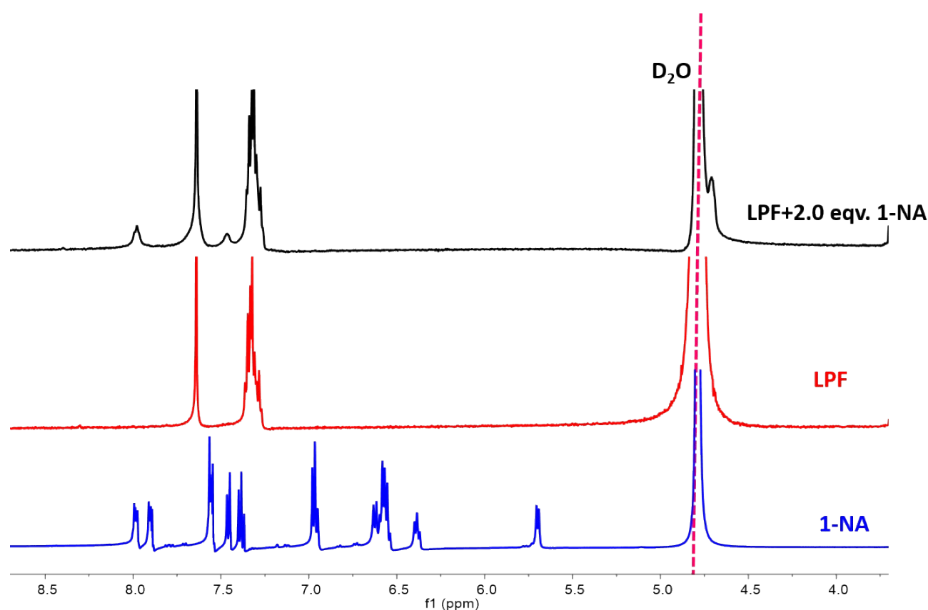


**Figure S11.**  $^1\text{H}$  NMR spectra of 1NA, LPF and LPF-1NA at molar ratios of 1:2 with the total gelators concentration of 0.2 wt% at room temperature.

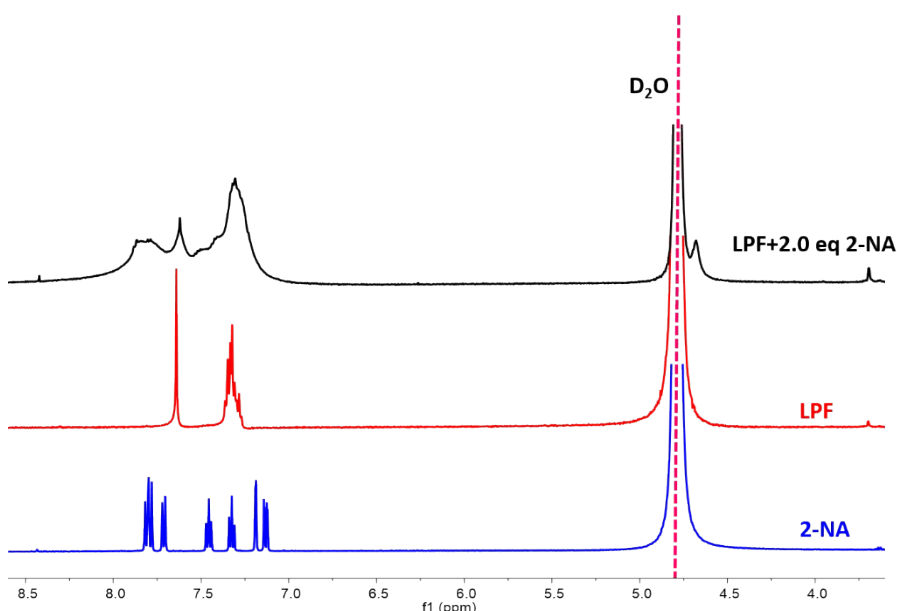


**Figure S12.**  $^1\text{H}$  NMR spectra of 2NA, LPF and LPF-2NA at molar ratios of 1:2 with the total gelators concentration of 0.2 wt% at room temperature.

## 2. Initial structure preparation

The initial structures of LPF-1NA and LPF-2NA supramolecular assemblies were prepared by substituting the para-ylene molecules in the reference structures from 1 with 1NA or 2NA.<sup>[1]</sup> The initial structures were constructed in a way by assuming potential formation of hydrogen bonds between the amine groups of NA molecules and original LPF-water assemblies. The c-dimensions of the original cells have been extended to 30 Å to eliminated periodicity long this dimension, while the periodicity along a- and b-dimensions are reserved. Geometry optimization (with convergence criteria set to that total energy <  $1 \times 10^{-4}$  kcal/mol, force < 0.005 kcal/mol/Å and maximum displacement <  $5 \times 10^{-5}$  Å) using the Forcite molecule of the Materials Studio package version 2017 were performed for initial structures, with optimized structures shown in Figure S13.

Then the initial structures were fed to the Forcite module of the Materials Studio package version 2017 to perform simulated annealing processes with distance constraints applied to the NA molecules. The positions of atoms in LPF molecules, water molecules were fixed to their original ones during the simulated annealing processes. The simulated annealing simulations were performed for 200 cycles from 10 to 600K with NVT ensemble. Each heating-cooling cycle lasts for 4ps (timestep = 2fs). By the end of each heating-cooling cycle, one structure will be generated, thus we will have 200 structures in total after each simulated annealing simulation. Without further notice, the forcefield used for both simulated geometry optimization and simulated annealing procedures is COMPASS II<sup>[2-3]</sup>.

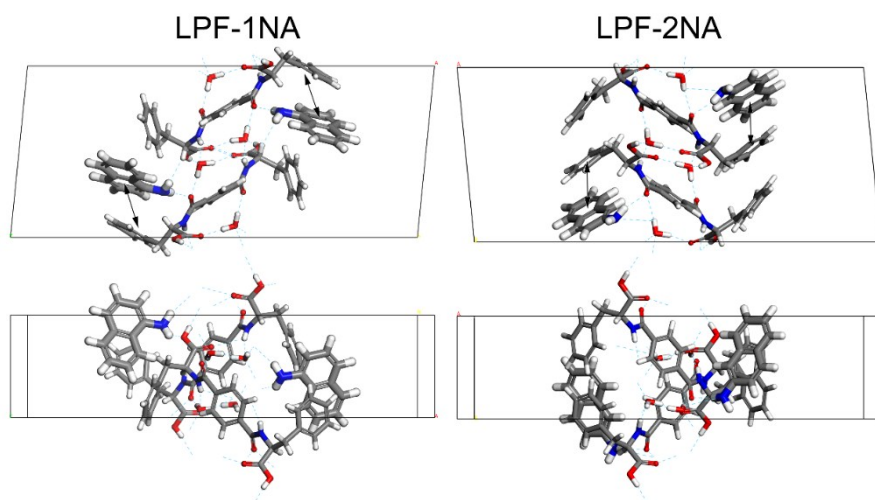


**Figure S13.** The initial optimized structures of LPF-1NA and LPF-2NA, the constraints to be applied in the subsequent simulated annealing processes were indicated by the black double arrows.

### 3. DFT optimized structures

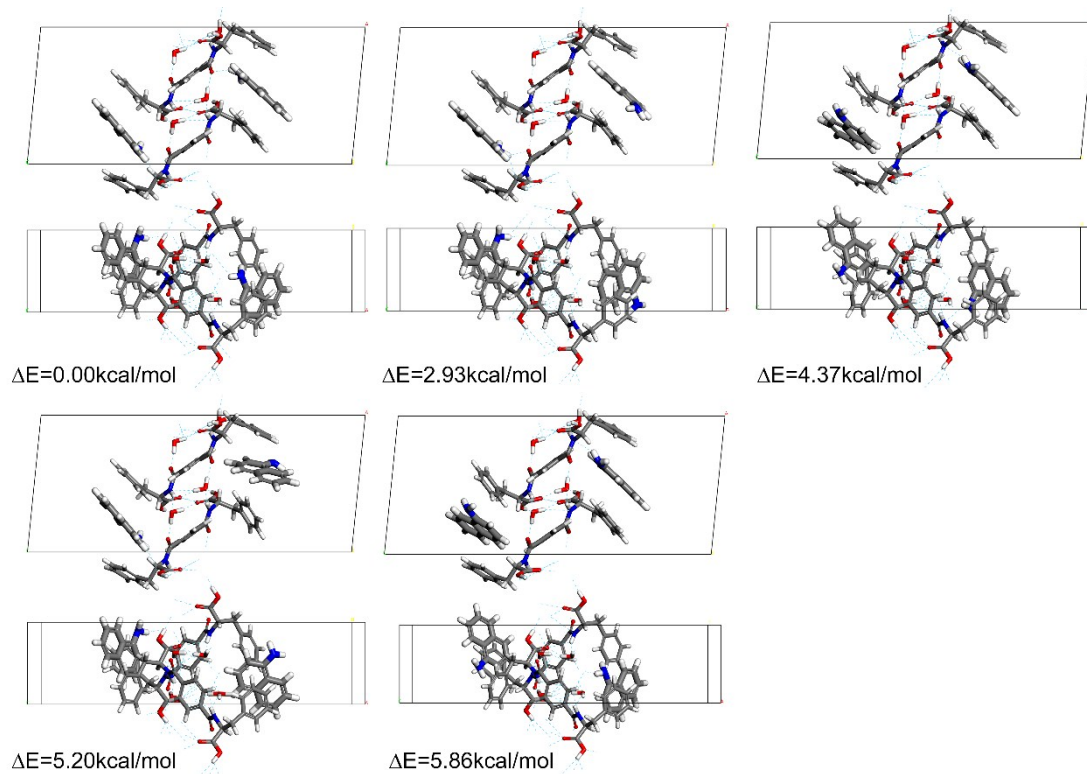


**Figure S14.** DFT optimized structures of LPF-1NA. Energy differences for each structure with respect to the lowest energy structure are also provided as references.

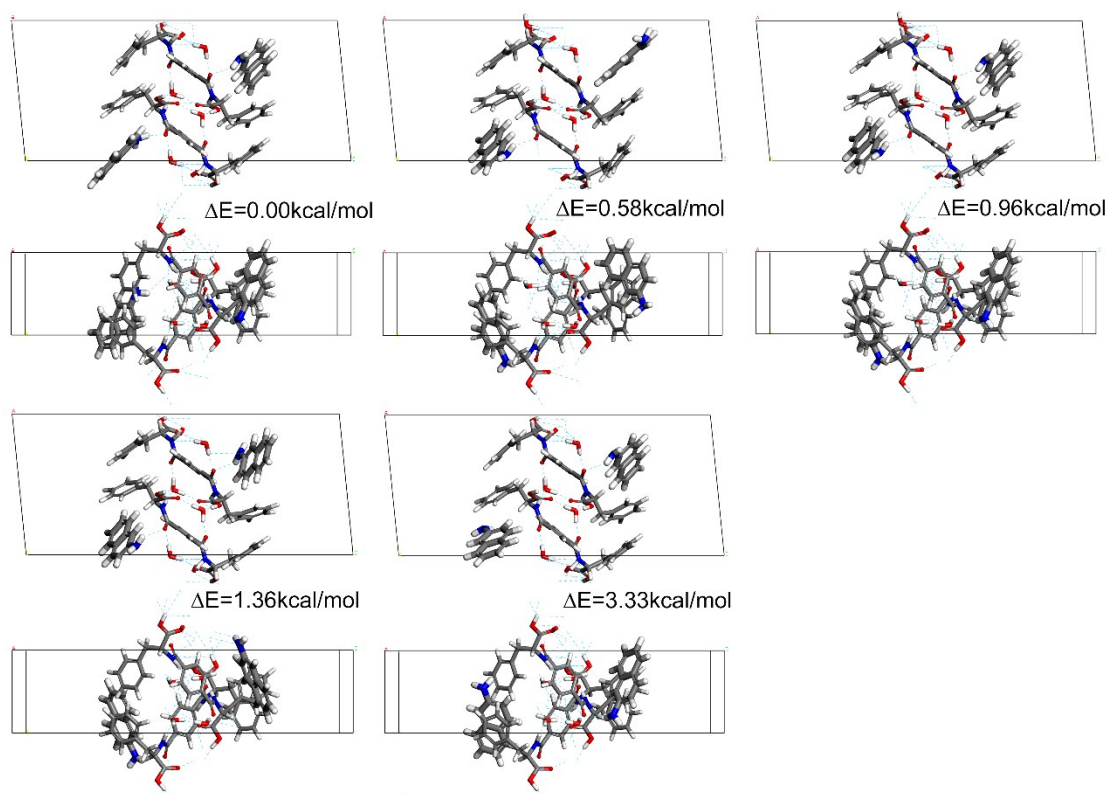


**Figure S15.** DFT optimized structures of LPF-2NA. Energy differences for each structure with respect to the lowest energy structure are also provided as references.

The top 5 low energy structures for both LPF-1NA and LPF-2NA are displayed in Figures 14 and 15. It is evident from the results of LPF-1NA that hydrogen bonds between amine groups in 1NA has important role in stabilizing the supramolecular assembly. Such hydrogen bond energy can be as high as about 3kcal/mol when comparing the lowest energy structure in Figure 14 with the second-lowest energy on showing only one 1NA can form hydrogen bond with the LPF-water assembly. It is also interesting to notice that further alignment of the naphthalene rings with the end phenyl rings in the case of LPF-1NA, suggesting possible stronger  $\pi$ - $\pi$  interactions. Moreover, the final lowest energy structure for LPF-1NA also tends to be more ordered as compared to the others, which is likely to lead to the more preferable structures. Considering distinct energy differences between different low energy structures, we chose the lowest energy structure for LPF-1NA for further VCD calculations. Further analysis of the lowest energy LPF-1NA structure shown in Figure 6 suggested the hydrogen bonds can form between amine group in 1NA molecule and ketone or carbonyl hydroxyl groups in LPF molecule. The hydrogen bonds formed has length of 2.5-2.9Å between LPF and 1NA molecules, showing moderate strength.

In the case of LPF-2NA as shown in Figure S15, 2NA molecules tend to be less well defined as compared to 1NA in LPF-1NA. Three out of five structures in LPF-2NA can be considered within the accuracy of DFT calculations ( $\Delta E < 1\text{kcal/mol}$ ). Further stabilization of the structures is attainable via  $\pi$ - $\pi$  interactions as suggested by the first 2 lowest energy structures, but none of them exhibit preferable hydrogen bonds in the 3rd lowest energy structure. Consider possible symmetry constraint then the NA molecules form supramolecular assemblies with LPF, we thus chose the 3rd lowest energy structure for further VCD calculation. A closer look at the optimized 3rd lowest energy structure in in Figure 6 indicate formation of hydrogen bonds between carbonyl groups in LPF and amine groups in 2NA. The hydrogen bonds in LPF-2NA supramolecular assembly are shown to have length around 2.3Å, indicating stronger hydrogen bonds formed as compared to those in LPF-1NA.

#### 4. DFT calculations of the VCD spectra



The candidate structures obtained through the strategy adopted in 2 were further fed to Gaussian 09<sup>[11]</sup> package in order to obtain their VCD spectra. The VCD spectra for both systems involved in this work were calculated at the B3LYP/6-31G(d,p) level with supramolecular structures extracted from their periodic cell without further geometry optimization. The VCD spectra were plotted using the MultiWFN<sup>[12]</sup> package version 3.6.

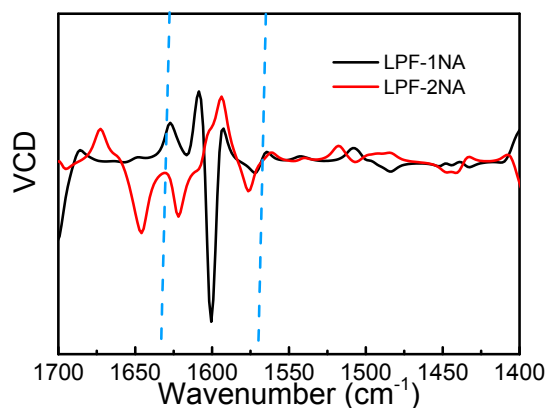


**Figure S16.** Calculated VCD spectra of cohydrogel of LPF-1NA/2NA.

## References

1. Liu, G.; Li, X.; Sheng, J.; Li, P.-Z.; Ong, W. K.; Phua, S. Z. F.; Ågren, H.; Zhu, L.; Zhao, Y. *ACS Nano*. **2017**, 11 (12), 11880-11889.
2. Sun, H., *The Journal of Physical Chemistry B* **1998**, 102 (38), 7338-7364.
3. Sun, H.; Jin, Z.; Yang, C.; Akkermans, R. L. C.; Robertson, S. H.; Spenley, N. A.; Miller, S.; Todd, S. M., *Journal of Molecular Modeling* **2016**, 22 (2), 47.
4. Aradi, B.; Hourahine, B.; Frauenheim, T., *The Journal of Physical Chemistry A*, **2007**, 111 (26), 5678-5684.
5. Elstner, M.; Porezag, D.; Jungnickel, G.; Elsner, J.; Haugk, M.; Frauenheim, T.; Suhai, S.; Seifert, G., *Physical Review B* **1998**, 58 (11), 7260-7268.
6. Goedecker, S.; Teter, M.; Hutter, J., *Physical Review B* **1996**, 54 (3), 1703-1710.
7. Hartwigsen, C.; Goedecker, S.; Hutter, J. *Physical Review B* **1998**, 58 (7), 3641-3662.
8. Krack, M., *Theoretical Chemistry Accounts* **2005**, 114 (1), 145-152.
9. Hutter, J.; Iannuzzi, M.; Schiffmann, F.; VandeVondele, J., *Computational Molecular Science* **2014**, 4 (1), 15-
10. Grimme, S.; Antony, J.; Ehrlich, S.; Krieg, H. *The Journal of Chemical Physics* **2010**, 132 (15), 154104.
11. Frisch, M. J.; Trucks, G. W.; Schlegel, H. B.; Scuseria, G. E.; Robb, M. A.; Cheeseman, J. R.; Scalmani, G.; Barone, V.; Mennucci, B.; Petersson, G. A.; Nakatsuji, H.; Caricato, M.; Li, X.; Hratchian, H. P.; Izmaylov, A. F.; Bloino, J.; Zheng, G.; Sonnenberg, J. L.; Hada, M.; Ehara, M.; Toyota, K.; Fukuda, R.; Hasegawa, J.; Ishida, M.; Nakajima, T.; Honda, Y.; Kitao, O.; Nakai, H.; Vreven, T.; Montgomery Jr., J. A.; Peralta, J. E.; Ogliaro, F.; Bearpark, M. J.; Heyd, J.; Brothers, E. N.; Kudin, K. N.; Staroverov, V. N.; Kobayashi, R.; Normand, J.; Raghavachari, K.; Rendell, A. P.; Burant, J. C.; Iyengar, S. S.; Tomasi, J.; Cossi, M.; Rega, N.; Millam, N. J.; Klene, M.; Knox, J. E.; Cross, J. B.; Bakken, V.; Adamo, C.; Jaramillo, J.; Gomperts, R.; Stratmann, R. E.; Yazyev, O.; Austin, A. J.; Cammi, R.; Pomelli, C.; Ochterski, J. W.; Martin, R. L.; Morokuma, K.; Zakrzewski, V. G.; Voth, G. A.; Salvador, P.; Dannenberg, J. J.; Dapprich, S.; Daniels, A. D.; Farkas, Ö.; Foresman, J. B.; Ortiz, J. V.; Cioslowski, J.; Fox, D. J. *Gaussian 09*, Gaussian, Inc.: Wallingford, CT, USA, 2009.
12. Lu, T.; Chen, F. *Journal of Computational Chemistry* **2012**, 33 (5), 580-592.